Effects of Neutrino Transport on the r-Process Nucleosynthesis for the Explosion of a 3.3 $M_\odot$ Helium Star

Motoaki SARUWATARI[1], Masa-aki HASHIMOTO[1] and Kenzo ARAI[2]

[1]*Department of Physics, Kyushu University, Fukuoka 810-8560*
[2]*Department of Physics, Kumamoto University, Kumamoto 860-8555*

(Received September 30, 2010)

We investigate r-process during the magnetohydrodynamical (MHD) explosion of supernova in a helium star of 3.3 $M_\odot$ with including the neutrino effects. Contrary to the case of the spherical explosion, jet-like explosion due to the combined effects of differential rotation and magnetic field reduces the electron fraction significantly inside the layers. It is found that the ejected material of low electron fraction responsible for the r-process comes out from just outside the neutrino sphere deep inside the Fe-core. This leads to the production of the second to third peaks in the solar r-process elements. We suggest that there are variations in synthesis of heavy elements according to the initial conditions of rotation and magnetic field. In particular, the third peak elements are significantly over-produced, indicating a possible new site of MHD jets in supernovae. We can infer that the third peak is originated from supernova explosions associated to the jet-like explosion such as γ-ray bursts.

§1. Introduction

The origin of heavy neutron-rich elements is mainly due to the r-process nucleosynthesis during the supernova explosions.[1)] The study of the r-process has been developed considerably keeping pace with the terrestrial experiments of nuclear physics far from the stability line of nuclides. In particular, among the three peaks ^{80}Se, ^{130}Te and ^{195}Pt in the abundance pattern of the r-elements in the solar system, the transition from the second to third peak elements has been advocated by nuclear physicists. Although supernovae are the most reliable astrophysical sites of the r-process,[2)] the explosion mechanism is still in debate. It has been believed that the explosion is triggered by the gravitational collapse of massive stars of $M > 10\ M_\odot$.[3)] It has been great hope that neutron-rich elements could be ejected during the shock wave propagation. As far as the one-dimensional calculations, almost all realistic numerical simulations concerning the collapse-driven supernovae have failed to explode the outer layer above the Fe-core due to drooping shock wave propagation.[4)] Therefore, a plausible site and mechanism of the r-process has not yet been clarified.

Explosive nucleosynthesis that produces most elements up to Fe-group nuclei has been calculated under the plausible assumption that the explosion is triggered from outside the Fe-core whose location is defined to be *mass cut*.[5)] The abundance pattern from C to Ge is rather consistent with the supernova observations, the chemical evolution of galaxies and the solar system abundances.[6)] Although this artificial explosion has succeeded in determining parameters to explain the observed light curves, the method cannot be applied to the r-process due to large electron fraction and low entropy above the *mass cut*.

During the development of many hydrodynamical simulations, nucleosynthesis in the jet-like explosion has been investigated with use of the two-dimensional (2D) hydrodynamical code.[7] It is found that the strong α-rich freeze out region forms after the shock wave passage. 2D magnetohydrodynamical (MHD) calculations have been performed under the various initial conditions concerning rotation and magnetic field.[8)–10)] The ZEUS-2D code[11)] has been modified to include a tabulated equation of state,[12)] electron captures and neutrino (ν-) transport.[8)]

It is found that for the cylindrical profiles of the rotation and magnetic field the shape of the shock wave becomes prolate compared to the case without magnetic fields though detailed studies on ν-transport must be developed. Furthermore, the confined magnetic fields behind the shock front push the shock wave strongly. It remains unclear whether some significant differences are found in MHD features if the initial models of stellar evolution include magnetorotational effects or not.[13)]

In the present paper, we perform MHD calculations of the explosion of a helium star of 3.3 $M_\odot$ untill the final simulation time $t_f \simeq 600$ ms. Two models are adopted for the initial configuration of rotation and magnetic fields. Contrary to the previous investigation of the r-process under adiabatic MHD explosion,[14)] we include the effects of neutrinos using a leakage scheme.[15)–17)] Moreover we examine possibility of the r-process in the MHD jets with use of our large nuclear reaction network.[18)]

§2. Supernova models

2.1. *MHD equations and neutrino processes*

Basic MHD equations are written as

$$\frac{D\rho}{Dt} + \rho\nabla\cdot\boldsymbol{v} = 0, \tag{2.1}$$

$$\rho\frac{D\boldsymbol{v}}{Dt} = -\nabla P - \rho\nabla\Phi + \frac{1}{4\pi}(\nabla\times\boldsymbol{B})\times\boldsymbol{B}, \tag{2.2}$$

$$\frac{\partial\boldsymbol{B}}{\partial t} = \nabla\times(\boldsymbol{v}\times\boldsymbol{B}), \tag{2.3}$$

$$\rho\frac{D(e/\rho)}{Dt} = -P\nabla\cdot\boldsymbol{v} + Q^+ - Q^-, \tag{2.4}$$

where D/Dt is the Lagrange derivative, ρ the density, $\boldsymbol{v}$ the velocity, P the pressure, $\boldsymbol{B}$ the magnetic field, e the internal energy density, Q^+ and Q^- are the ν- heating and cooling rates, respectively. The gravitational potential Φ is determined from the Poisson equation.

Neutrino luminosity L_ν is evaluated from the average ν-energy $\bar{\epsilon}_{\nu,\mathrm{esc}}$ (see Eq. (2.16) below) that escapes freely:

$$L_\nu = \int_V \bar{\epsilon}_{\nu,\mathrm{esc}}\frac{n_\nu}{\tau_{\mathrm{esc}}}dV, \tag{2.5}$$

where n_ν is the ν-number density and τ_{esc} is the escape time for a neutrino to reach the ν-sphere R_ν that is obtained from the leakage scheme[17)] in terms of the ν-mean

free path λ_{tot} as

$$\int_{R_\nu}^{\infty} \frac{dr}{\lambda_{tot}} = \frac{2}{3}. \tag{2.6}$$

Contrary to the original leakage scheme, we do not adopt free stream approximation for neutrinos outside R_ν. We consider the fact that for each time step of Δt, neutrinos run by $c\Delta$t, which is typically 10^4 cm in our simulations.

We evaluate Q^+ and Q^- as[19]

$$Q^+ = \sigma_{ab} n_n \frac{L_\nu}{4\pi r^2}, \qquad Q^- = \bar{\epsilon}_{\nu,\mathrm{esc}} \frac{n_\nu}{\tau_{\mathrm{esc}}}, \tag{2.7}$$

where n_n is the number density of free neutrons and σ_{ab} is the ν-absorption cross section by free neutrons that is the most important heating source.

The change in Y_e is governed by ν-interactions with protons and nuclei as

$$\frac{dY_e}{dt} = -\Gamma_p Y_p - \Gamma_N Y_N. \tag{2.8}$$

The electron capture rate by a proton ($p + e^- \longrightarrow n + \nu_e$) with $Q_p = 1.3$ MeV is

$$\Gamma_p = \frac{1}{2\pi^3\hbar} \frac{G_F^2 C_V^2 (1+3a^2)}{(h^3c^3)^2} I_p, \tag{2.9}$$

$$I_p = \int_Q^{\mu_e} dE_e E_e^2 E_\nu^l f_e (1 - f_\nu). \tag{2.10}$$

Here G_F is the Fermi coupling constant, $C_V = 0.97$ is the pseudo vector coupling constant, $l = 2$, $Q = Q_p + \mu_\nu$ and f_α is the Fermi-Dirac distribution of particles α

$$f_\alpha = \frac{1}{1 + e^{(\epsilon_\alpha - \mu_\alpha)/T_\alpha}} \qquad \text{for } \alpha = e,\ \nu, \tag{2.11}$$

where ϵ_α and μ_α are the single particle energy and the chemical potential, respectively, in units of the Boltzmann constant. We note that outside the equilibrium region of neutrinos and baryons, significant thermal deviation comes out, i.e., $T_\nu \neq T_m$. The electron capture rate by a nucleus of the atomic number Z with Q_N is

$$\Gamma_N = \frac{12}{7} \frac{1}{2\pi^3\hbar} \frac{G_F^2 C_A^2 (Z-20)}{(h^3c^3)^2} I_N, \tag{2.12}$$

where I_N is obtained from Eq. (2.10) with $l = 2$ and $Q = Q_N + \mu_\nu$, C_A is the axial vector coupling constant. We set $|C_A/C_V| = 1.27$. Note that this capture process is inhibited above the neutron number $N = 40$ due to the effects of shell-blocking.[20]

Energies of emitted neutrinos by the individual electron captures are[21]

$$E_{\nu,p} = \frac{J_p}{I_p}, \qquad E_{\nu,N} = \frac{J_N}{I_N}, \tag{2.13}$$

where J_p and J_N are obtained from I_p and I_N, respectively, with $l = 3$. The average energy of neutrinos emitted by electron captures are written as

$$\bar{\epsilon}_\nu = \frac{E_{\nu,p}\dot{Y}_p + E_{\nu,N}\dot{Y}_N}{\dot{Y}_p + \dot{Y}_N}, \tag{2.14}$$

where Y_p, Y_N and Y_e are the number fractions of protons, nuclei and electrons, relative to baryons. This average energy is added to obtain the ν-energy density at the next time step in our simulations.

Inside the ν-sphere, T_ν and μ_ν are evaluated in terms of n_ν and the ν-energy density e_ν

$$n_\nu = \frac{T_\nu^3}{(\hbar c)^3}\int 4\pi\epsilon_\nu^2 f_\nu d\epsilon_\nu, \qquad e_\nu = \frac{T_\nu^4}{(\hbar c)^3}\int 4\pi\epsilon_\nu^3 f_\nu d\epsilon_\nu, \tag{2.15}$$

where the Fermi-Dirac distribution is assumed for neutrinos. Outside the ν-sphere, neutrino radiation can be approximated as the black body with $\mu_\nu = 0$. The average ν-energy is written as

$$\bar{\epsilon}_{\nu,\mathrm{esc}} = \frac{F_3}{F_2}T_{\nu,\mathrm{sp}}, \tag{2.16}$$

where $T_{\nu,\mathrm{sp}}$ is the ν-temperature at the ν-sphere and the Fermi integral F_i is obtained from

$$F_i = \int_0^\infty \frac{x^i}{1+e^x}dx \qquad \text{for } i = 1,\ 2. \tag{2.17}$$

If $T_\nu \geq T_m$ inside the ν-sphere, the baryon energy density e_m increases due to the energy flow from neutrinos

$$\frac{de_m}{dt} = \frac{c}{\lambda_\nu}e_\nu, \tag{2.18}$$

where λ_ν is the mean free path of neutrinos.[22] In this region, we replace $T_{\nu,\mathrm{sp}}$ by T_m to get $\bar{\epsilon}_{\nu,\mathrm{esc}}$ in Eq. (2.16) to avoid numerical problems, which would be underestimate of ν-energy.

The similar procedure can be applied to anti-neutrinos of the reaction, $n + e^+ \longrightarrow p + \bar{\nu}_e$, with the substitutions

$$\mu_e \longrightarrow -\mu_e, \quad \mu_\nu \longrightarrow \mu_{\bar{\nu}}, \quad T_\nu \longrightarrow T_{\bar{\nu}}. \tag{2.19}$$

We include the effects of other ν-processes in Eq. (2.4). They are

$$e^+ + e^- \longrightarrow \nu_x + \bar{\nu}_x,$$
$$\gamma \longrightarrow \nu_x + \bar{\nu}_x$$

for three flabors of neutrinos, $x = e$, τ and μ. These processes are important in the late stage of the explosion. Almost all ν-luminosity at this stage is supplied by these processes. The reaction rates are given in Ref. 16). Electron neutrinos contribute

both cooling and heating. On the other hand, μ and τ neutrinos do only cooling. The emission rate of ν_e and $\overline{\nu}_e$ by electron-positron pair annihilation is given by

$$R_{ee}(\nu_e,\overline{\nu}_e) = \frac{(C_1+C_2)_{\nu_e,\overline{\nu}_e}}{36}\frac{\sigma_0 c}{(m_e c^2)^2}\epsilon_{e^-}\epsilon_{e^+}(1-f_{\nu_e}(\epsilon))_{ee}(1-f_{\overline{\nu}_e}(\epsilon))_{ee}, \quad (2.20)$$

where $\sigma_0 = 1.76\times10^{-44}\mathrm{cm}^2$ and ϵ_{e^-} and ϵ_{e^+} indicate energy densities of electrons and positrons. The weak interaction constants are $(C_1+C_2) = (C_V-C_A)^2+(C_V+C_A)^2$. The blocking factor $(1-f_{\nu_e}(\epsilon))_{ee}$ in the neutrino phase space is approximately written as

$$(1-f_{\nu_i}(\epsilon))_{ee} = \left[1+\exp\left(-\left(\frac{1}{2}\frac{F_4(\eta_e)}{F_3(\eta_e)}+\frac{1}{2}\frac{F_4(-\eta_e)}{F_3(-\eta_e)}-\eta_{\nu_i}\right)\right)\right]^{-1}, \quad (2.21)$$

where $F_n(\eta)$ is the Fermi integral

$$F_n(\eta) = \frac{T^{n+1}}{(\hbar c)^{n+1}}\int_\eta^\infty \frac{x^n}{1-e^{x-\eta}}dx \qquad \text{for } n=3,\ 4 \quad (2.22)$$

with $\eta = \mu_e/T$.

For the production of $(\nu_\mu,\ \overline{\nu}_\mu)$ and $(\nu_\tau,\overline{\nu}_\tau)$, the corresponding rate is

$$R_{ee}(\nu_x) = \frac{(C_1+C_2)_{\nu_x,\overline{\nu_x}}}{9}\frac{\sigma_0 c}{(m_e c^2)^2}\epsilon_{e^-}\epsilon_{e^+}(1-f_{\nu_x}(\epsilon))^2_{ee}, \quad (2.23)$$

where $(C_1+C_2)_{\nu_x,\overline{\nu}_x} = (C_V-C_A)^2+(C_V+C_A-2)^2$. The rate of creation of ν_e or $\overline{\nu}_e$ by the decay of transversal plasmons can be written with sufficient accuracy as

$$R_\gamma(\nu_e,\overline{\nu}_e) = \frac{\pi^3}{3\alpha^*}C_V^2\frac{\sigma_0 c^2}{(m_e c^2)^2}\frac{T^8}{(hc)^6}\gamma^6\exp(-\gamma)(1+\gamma)(1-f_{\nu_e}(\epsilon))_\gamma(1-f_{\overline{\nu_e}}(\epsilon))_\gamma \quad (2.24)$$

and the corresponding rate for producing ν_x is

$$R_\gamma(\nu_x,\overline{\nu}_x) = \frac{4\pi^3}{3\alpha^*}(C_V-1)^2\frac{\sigma_0 c^2}{(m_e c^2)^2}\frac{T^8}{(hc)^6}\gamma^6\exp(-\gamma)(1+\gamma)(1-f_{\nu_x})_\gamma, \quad (2.25)$$

where α^* is the fine-structure constant, $\gamma = 5.5565\times10^{-2}\sqrt{(\pi^2+3\eta_e^2)/3}$ and the blocking factor

$$(1-f_{\nu_x})_\gamma = \left[1+\exp\left(-\left(1+\frac{1}{2}\frac{\gamma^2}{1+\gamma}-\eta_{\nu_i}\right)\right)\right]^{-1}. \quad (2.26)$$

Outside R_ν, we include the terms of ν-radiation in Eq. (2.8) as

$$\frac{dY_e}{dt} = -\Gamma_p Y_p - \Gamma_N Y_N + \frac{c}{\lambda_\nu} - \frac{c}{\lambda_{\overline{\nu}}}Y_n, \quad (2.27)$$

where λ_ν and $\lambda_{\overline{\nu}}$ are the mean free paths of electron neutrinos and anti-neutrinos.

Table I. Initial parameters of pre-collapse models.

Model	$T/\|W\|$ (%)	$E_m/\|W\|$ (%)	X_0 (10^8 cm)	Z_0 (10^8 cm)	Ω_0 (s^{-1})	B_0 (G)
model A	0.5	0.1	0.1	1	42.9	5.2×10^{13}
model B	1.5	0.1	0.1	1	72.9	5.2×10^{13}

2.2. *Initial models*

A presupernova model is calculated from the evolution of a He-core of 3.3 $M_\odot$ that corresponds to 13 $M_\odot$ in the main sequence stage.[3] The mass of the Fe-core is 1.18 $M_\odot$ that is the smallest Fe-core in massive stars obtained from the stellar evolution calculations with the limitation of spherical symmetry. The radius of the Fe-core that has steep density gradient is $R = 8.50 \times 10^7$ cm. The mass of the Si-rich layer is 0.33 $M_\odot$ and the layer extends to 5.47×10^8 cm above the Fe-core. When density exceeds $\rho = 2.79 \times 10^{10}$ g cm^{-3} and temperature is $T = 9.04 \times 10^9$ K, the Fe-core begins to collapse, implying the transition from the hydrostatical to hydrodynamical stage.

The initial pre-collapse models are constructed by using the density and temperature distributions of the original Fe+Si core. We specify cylindrical properties of the angular velocity Ω and the toroidal component of the magnetic field B_ϕ as follows:[8]

$$\Omega(X,Z) = \Omega_0 \frac{X_0^2}{X^2+X_0^2}\frac{Z_0^4}{Z^4+Z_0^4}, \quad B_\phi(X,Z) = B_0 \frac{X_0^2}{X^2+X_0^2}\frac{Z_0^4}{Z^4+Z_0^4}, \tag{2.28}$$

where X and Z are the distances from the rotational axis and the equatorial plane with X_0, Z_0, Ω_0 and B_0 being model parameters. The initial parameters of models are given in Table I, where T is the rotational energy, E_m is the magnetic energy and W is the gravitational energy. Note that model A contains a rapidly rotating core and strong magnetic field. Model B represents an extreme case with very rapid rotation and strong magnetic field. In all our computations, spherical coordinates (r, θ) are adopted. The computational region is set to be $0 \le r \le 4000$ km and $0 \le \theta \le \pi/2$, where the mass included in the pre-collapse models amounts to 1.42 $M_\odot$. The first quadrant of the meridian section is covered with 300 (r) × 30 (θ) mesh points. To get information of mass elements, ten thousand tracer particles are placed within the region of $0.449 \le Y_e \le 0.49$ between 0.8 $M_\odot$ ($r = 410$ km) and 1.3 $M_\odot$ ($r = 2200$ km).

Table II. Crucial quantities for the collapse-driven supernova simulations*r*-process. t_b is the time at the bounce and t_f is the final time.

Model	t_b (ms)	t_f (ms)	$T/\|W\|_f$ (%)	$E_m/\|W\|_f$ (%)	$E_{\rm exp}$ (10^{51} erg)	$M_{\rm ej}$ ($M_\odot$)
model A	133	433	8.80	0.142	1.13	0.111
model B	180	624	15.3	0.339	0.484	0.022

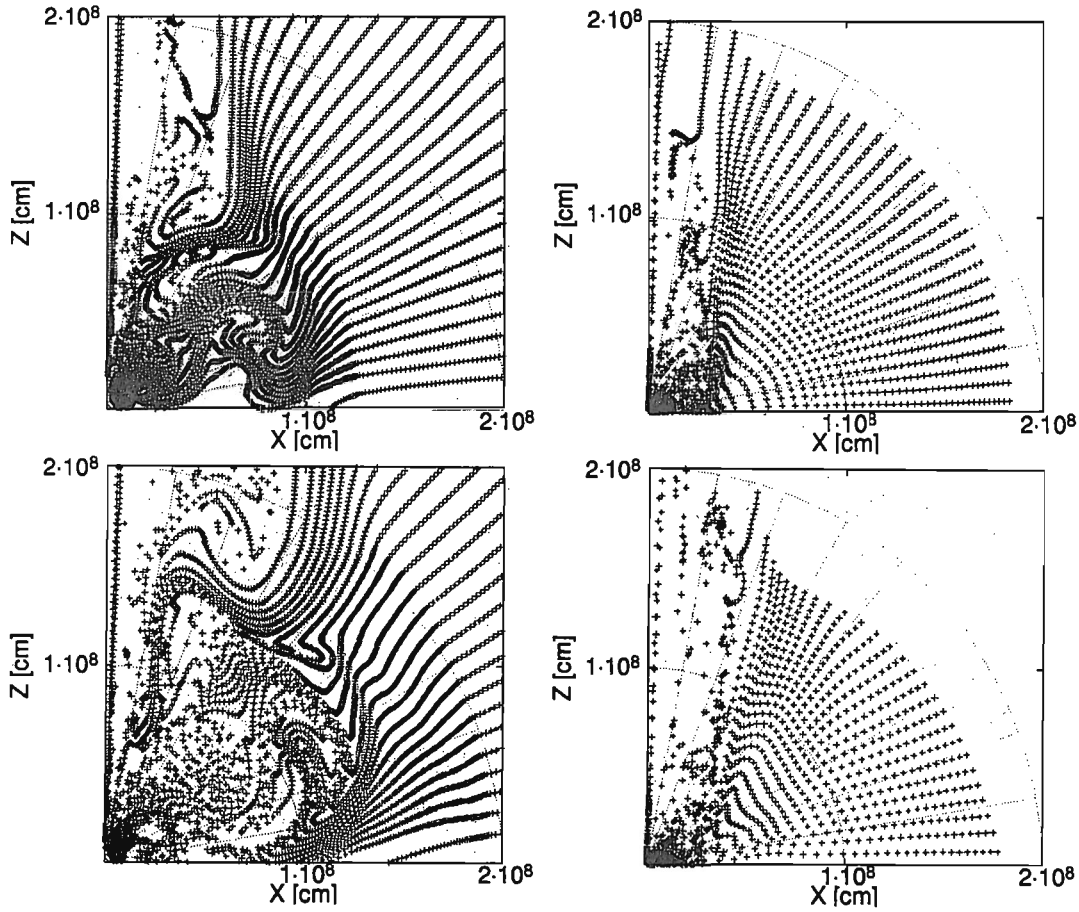

Fig. 1. Snapshots of tracer particles at $t = 100$ ms (top) and $t = 200$ ms (bottom) after the bounce in models A (left) and B (right).

§3. Explosion models

We perform calculations of the collapse, bounce and propagation of the shock wave with use of ZEUS-2D where the realistic equation of state[12] has been implemented.[8] It is noted that the contribution of the nuclear energy generation is usually negligible compared to the shock energy. Our results of MHD calculations are summarized in Table II, where $E_{\rm exp}$ is the explosion energy when the shock reaches the edge of the Fe-core[10] and $M_{\rm ej}$ is the mass summed over the ejected tracer particles. It does not always depend on $T/|W|$ and/or $E_m/|W|$ whether the explosion succeeds or not. While the jet-like explosion occurs along the equator (up to 40° from the equator) in model A, a collimated jet emerges from the rotational axis in model B (Fig. 1). A proto-neutron star remains after the jet-like explosion. The masses are 1.01 and 1.12 $M_\odot$ for models A and B, respectively, inside the radius 300 km. During the explosion, temperature exceeds 10^{10} K around the original layers of the Si+Fe core, where the nuclear statistical equilibrium (NSE) is realized.

As seen from Fig. 1 the equatorial region is ejected in model A with rather high

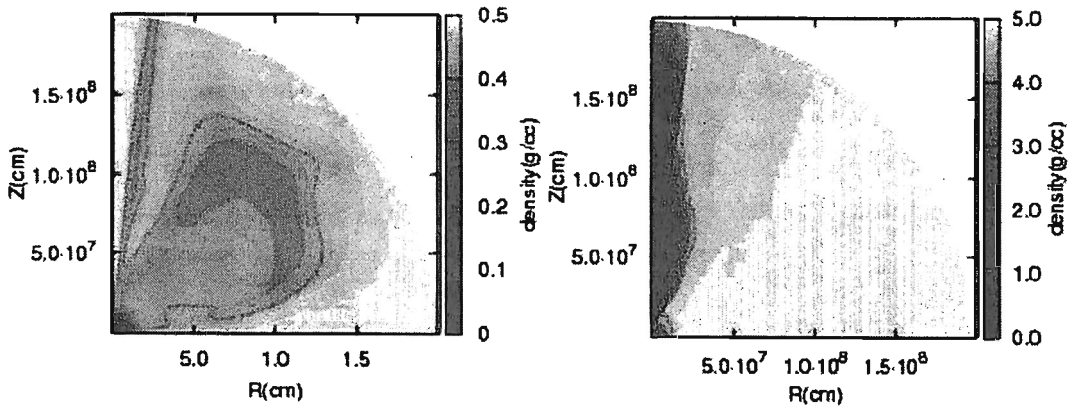

Fig. 2. Contour of Y_e over the range 0.1 – 0.5 at final stage of calculation in models A (left) and B (right).

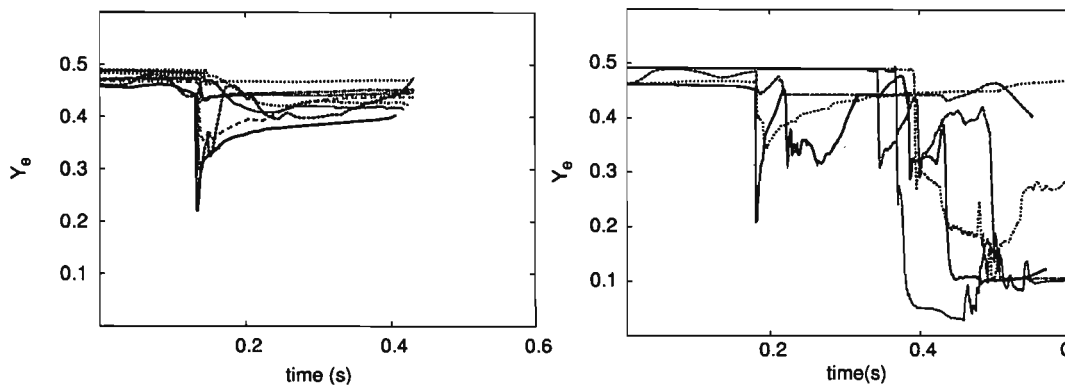

Fig. 3. Evolution of Y_e in models A (left) and B (right).

value of $Y_e \simeq 0.50$ (Fig. 2). In model B, materials are ejected as the jets along the polar regions where total angle is collimated around 20° from the axis (see the right panel in Fig. 1) The corresponding evolutions of Y_e relevant to the r-process are shown in Fig. 3. The lowest value of $Y_e \simeq 0.20$ is found around the polar region as seen in the right panel of Fig. 2.

Figure 4 shows the ejected mass against Y_e in the range $0.05 \leq Y_e \leq 0.50$. In model A the ejection for $Y_e > 0.40$ comes from the Si-rich layer along the equatorial region, which is attributed to strong centrifugal force relative to magnetic one. We recognize that as against the spherical explosion, Y_e decreases significantly in jet-like explosion of model B.

§4. Nuclear reaction network for the r process nucleosynthesis

We calculate the r-process nucleosynthesis for the explosion model B. We have developed the nuclear reaction network that had been constructed for the r-process

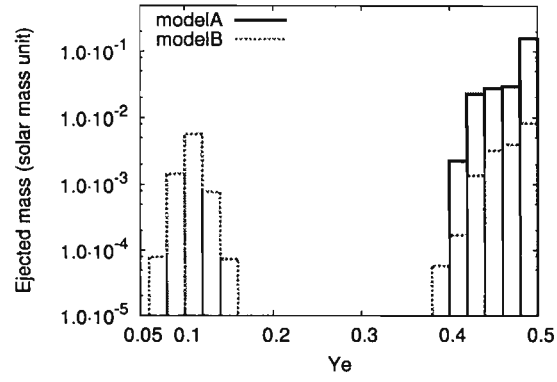

Fig. 4. Ejected mass as a function of Y_e in models A (thick line) and B (dotted line).

based on Ref. 14). The network has been extended toward the neutron-rich side toward the neutron-drip line. The full network consists of about 4000 nuclear species up to $Z = 100$. We include two body reactions, (n,γ), (p,γ), (α,γ), (p,n), (α,p), (α,n) and their inverses. We construct two kinds of the network, called FRDM and ETFSI. The mass formula of FRDM is constructed by the Nilsson-Struntinsky model considering effects of shell and microscopic part. ETFSI approach is a semi-classical approximation to the Hartree-Fock method in which the shell corrections are calculated with the integral version of the Strutinsky theorem. Most reaction rates are taken from experimental ones if avairable which are supplemented by theoretical data with inverse reaction rates and partition functions with use of FRDM or ETFSI.

When $T > 10^{10}$ K, all nuclei are assumed to be in NSE.[14),18)] The NSE code is used just after the temperature drops 10^{10} K until around 9×10^9 K. Then the nuclear reaction network of the r-process has been operated till the temperature decreases to $2 - 3 \times 10^9$ K ($t \simeq 600$ ms) using the data of the MHD calculations. After this epoch, network calculations are performed until $T \simeq 10^7$ K ($t \simeq 10$ s) with the method described in Ref. 14).

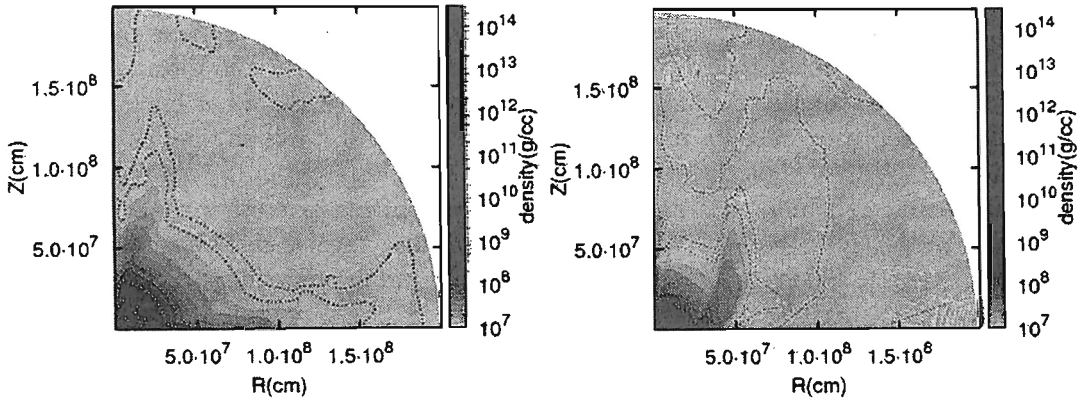

Fig. 5. Density contour over $10^8 - 10^{14}$ g cm^{-3} at $t = 200$ ms after the bounce in models A (left) and B (right).

§5. Discussions

We can indicate the possibility of the r-process nucleosynthesis during MHD explosion in a massive star of 13 $M_{\odot}$, where we have examined two pre-collapse models. They have been constructed changing the artificial distributions of rotation and magnetic fields parametrically.[14)]

We include the effects of neutrinos by using the leakage scheme. This scheme treats the neutrino effects approximately and assumes the Fermi-Dirac distribution for neutrinos. Other schemes are developed for solving neutrino transport in recent researches. For example, an isotropic diffusion source approximation scheme solves the Boltzmann equation approximately and obtains the consistent results with 1D simulations. We will use it in future work.

In case of the rapid rotation and strong magnetic field (model A), jet like explosion is obtained in the direction of the equatorial region (the left panel in Fig. 5). It is, however, impossible to reproduce the r-elements even up to the second peak of the solar r-process abundance pattern, because Y_e of the ejected materials distributes in the range of high values of $Y_e \geq 0.4$. In model B, where we have adopted a special initial configuration of concentrated magnetic field with strong differential rotation, the jet-like explosion emerges in the direction of the rotational axis (the right panel in Fig. 5). The difference is ascribed to the fact that model B has larger value of the angular velocity compared to model A by a factor of 1.7. We compared the produced heavy elements with the solar r-elements in Fig. 6, where the results for two different mass formulae are shown. The model B may present an appropriate site for reproducing only the third peak with the first and second peaks under-produced. Contrary to the negative conclusion against the possible r-process in the previous study,[14)] we have succeeded in reproducing the distributions of the r-elements as far as the third peak of the solar pattern is concerned. At the same time, we have proposed the possibility for the lower Y_e materials to be ejected significantly if the neutrino transport works appropriately.

Observations of γ-ray bursts associated with supernovae are rare at the present observations. Therefore, the new site of the r-process to produce only the third peak of the solar pattern should be also rare not to conflict with the chemical evolution of galaxies. The nuclear process after the third peak would have some relations to our MHD jet model. Since γ-ray bursts have continued from the formation of the first star, a new model beyond our jet model would give a clue of nuclear cosmochronology represented by a nucleus of ^{232}Th whose half life is as long as the age of the universe.[23)]

We could conclude that supernova explosions of massive stars associated with the r-process could come true if a progenitor has special distributions of rotational/magnetic fields inside the stellar core and simple neutrino transport scheme like leakage one can be applied.

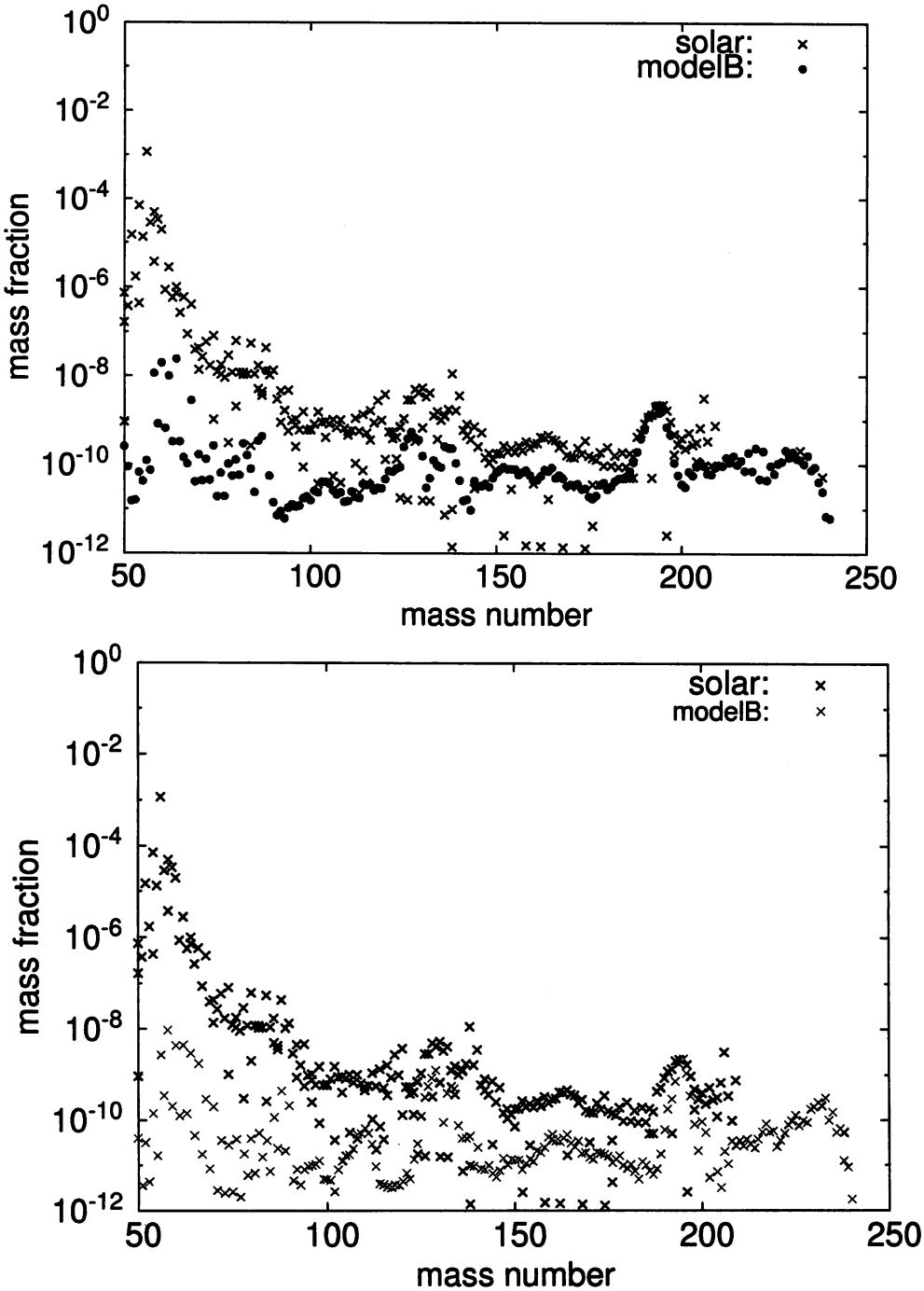

Fig. 6. Mass fractions of r-process nucleosynthesis in model B using ETFSI (upper) and FRDM (lower). The third peak is reproduced for both mass formulae.

Acknowledgements

This work has been supported in part by a Grant-in-Aid for Scientific Research (19104006, 21540272) of the Ministry of Education, Culture, Sports, Science and Technology of Japan.

References

1) F.-K. Thielemann et al. Proc. of 1CRC 2001: 1©Copernicus Gesellschaft 2001.
K. Sato, Prog. Theore. Phys. **51** (1974), 726.
P. A. Seeger, W. A. Fowler and D. D. Clayton, Astrophys. J. **11** (1965), 121.
Y.-Z. Qian, Prog. Part. Nucl. Phys. **50** (2003), 153.
2) Y.-Z. Qian, First Argonne/MSU/JINA/INT RIA Wokshop (2005).
3) M. Hashimoto, Prog. Theor. Phys. **94** (1995), 663.
4) H.-Th. Janka et al. IAU Coll. 192, in press (astro-ph/0401461).
5) F.-K. Thielemann, K. Nomoto and M. Hashimoto, Astrophys. J. **460** (1996), 408.
M. Hashimoto, K. Nomoto and T. Shigeyama, Astron. Astrophys. **210** (1989), L5.
6) F. X. Timmes, S. E. Woosley and T. A. Weaver, Astrophys. J. **98** (1995), 617.
T. Tsujimoto, K. Iwamoto, M. Hashimoto, K. Nomoto and F.-K. Thielemann, *Origin and Evolution of the Elements*, (World Scientific, 1993) p. 50.
7) S. Nagataki, M. Hashimoto, K. Sato and S. Yamada, Astrophys. J. **486** (1997), 1026.
8) K. Kotake, H. Sawai, S. Yamada and K. Sato, Astrophys. J. **608** (2004), 391.
9) K. Kotake, S. Yamada, K. Sato, K. Sumiyoshi, H. Ono and H. Suzuki, Phys. Rev. D **609** (2004), 124004.
S. Yamada, K. Kotake and T.Yamasaki, New. J. Phys. **6** (2004), 79.
T. Takiwaki, K. Kotake, S. Nagataki and K. Sato, Astrophys. J. **616** (2004), 1086.
10) S. Yamada and H. Sawai, Astrophys. J. **608** (2004), 907.
11) J. M. Stone and M. L. Norman, Astrophys. J. **80** (1992), 791.
12) H. Shen, H. Toki, K. Oyamatsu and K. Sumiyoshi, Nucl. Phys. A **637** (1998), 435.
13) S. E. Woosley and T. A. Weaver, Astrophys. J. **101** (1995), 181.
A. Heger, S. E. Woosley, N. Langer and H. C. Spruit, in IAU Symp. 215, Stellar Rotaion, in press (astro-ph/0301374).
14) S. Nishimura, K. Kotake, M. Hashimoto, S. Yamada, N. Nishimura, S. Fujimoto and K. Sato, Astrophys. J. **642** (2006), 410.
15) R. Epstein, Astrophys. J, **223** (1978). 1037.
K. A. van Riper and J. M. Lattimer, Astrophys. J. **249** (1981), 270.
16) M. Ruffert, H.-Th. Janka and G. Schafer, Astron. Astrophys. 311 (1996), 532.
17) K. Kotake, S. Yamada and K. Sato, Astrophys. J, **595** (2003), 304.
18) M. Ono, M. Hashimoto, S. Fujimoto, K. Kotake and S. Yamada, Prog.Theor.Phys. **122** (2009), 755.
19) H. A. Bethe, Rev. Mod. Phys. **62** (1990), 801.
H.-T. Janka, Astron. Astrophys. **368** (2001), 527.
20) G. M. Fuller, W. A.Fowler and M. J. Newmann, Astrophys. J. **252** (1982), 715.
k. Langanke et al. Phys. Rev. Lett. **90** (2003), 241102.
21) R. I. Epstein and C. J. Pethick, Astrophys. J. **243** (1981), 1003. —— S. L. Shapiro and S. A. Teukolsky, Black Holes, White Dwarfs, and Neutron Stars (Wiley, 1983).
22) D. L. Tubbs and D. N. Schramm, Astrophys. J. **201** (1975), 467.
23) D. D. Clayton, Principles of Stellar Evolution and Nucleosynthesis (New York: McGraw-Hill, 1968).